Physica 29D (1987) 181–190
North-Holland, Amsterdam

ANALYTICAL DETERMINATION OF UNSTABLE PERIODIC ORBITS IN AREA PRESERVING MAPS

G.L. DA SILVA RITTER and A.M. OZORIO DE ALMEIDA
Instituto de Física, UNICAMP, Campinas, 13081 SP, Brazil

and

R. DOUADY
Centre de Mathématiques, Ecole Polytechnique, 91128 Palaiseau Cedex, France

Received 2 April 1987
Revised manuscript received 4 June 1987

The Birkhoff normal form, for the neighbourhood of an unstable fixed point of an analytical area preserving map, was proved by Moser to converge. We here show that the region of convergence in fact stretches along a narrow strip surrounding the stable and the unstable manifolds. Consequently the normal form can be used to compute homoclinic points and unstable periodic orbit families that accumulate on them. This is verified for quadratic maps: we find unstable orbits which return to themselves within an accuracy of twenty-one significant figures.

A pair of linear equations is derived, which supply approximately all the periodic orbits accumulating on a given homoclinic point. This explicit formula is asymptotically valid in the limit of large periods.

1. Introduction

The Birkhoff normal form is a simplification of an area preserving map, brought about by a coordinate transformation specified by a formal series. Birkhoff presented in 1920 versions for both linearly stable and unstable fixed points [1]. However, the former have received by far the greater attention, in spite of being beset by small denominators and representing an oversimplified representation of the motion. None of these problems arise for the unstable (hyperbolic) points. The normal map is very similar to the linearized map, to which the map is conjugate by a homeomorphism in a neighbourhood of any hyperbolic point, according to the Hartman–Grobman theorem [2]. In fact the convergence of the formal series was proved by Moser in 1956 [3]. The problem has been simply one of relevance: why bother to compute an analytical form for a small region which most points will visit for only a few iterations of the map?

The reason is that the region of convergence of the normal form actually reaches out along the stable and unstable manifolds. It may thus become practicable to work with a truncation of the series as far as one or more *homoclinic points*, i.e. points of transverse intersection of the stable and the unstable manifolds. The verification, that precise computations of homoclinic points in this manner could be achieved, was the subject of a preliminary report [4]. The great advantage of this method over a direct computation is that it provides the entire homoclinic orbit (an infinite number of points) with uniform precision. In this paper we prove that the primitive neighbourhood of convergence established by Moser can indeed be extended indefinitely along the separatrices.

The region of convergence for the normal form also includes hyperbolae near the separatrices.

Their image by the normal form transformation are open invariant curves that self-intersect near the homoclinic points. Following the orbits of these points of self-interaction we meet with periodic orbits of arbitrarily large period. We have used exactly this method to calculate periodic orbits of quadratic maps to a very high accuracy.

The periodic orbits of higher and higher period accumulate on the homoclinic point. We thus obtain explicity linear equations for high order periodic points, by linearizing the normal form transformation in the neighbourhood of the homoclinic point. All the periodic points which accumulate on a given homoclinic point can be obtained in this simple way. The explicit formulae hold asymptotically in the limit where the number of periodic points of the orbit lying on each invariant curve is infinite.

2. Convergence of the normal form

Consider an area preserving map f: $\mathrm{R}^2 \to \mathrm{R}^2$, in which the origin is an unstable fixed point and the components of the vector functions $f(x)$ and $f^{-1}(x)$ are analytic functions on the whole plane. A linear area preserving (symplectic) transformation exists which takes the map into the form

$$\begin{aligned} x_1' &= \lambda x_1 + \sum_{k=2}^{\infty} \sum_{l=0}^{k} f_{1kl} x_1^{k-l} x_2^l, \\ x_2' &= \lambda^{-1} x_2 + \sum_{k=2}^{\infty} \sum_{l=0}^{k} f_{2kl} x_1^{k-l} x_2^l. \end{aligned} \tag{1}$$

Then according to the *Birkhoff–Moser theorem* [3], there exists a transformation N: $\mathrm{R}^2 \to \mathrm{R}^2$ with equations

$$\begin{aligned} x_1 &= X_1 + \sum_{k=2}^{\infty} \sum_{l=0}^{k} N_{1kl} X_1^{k-l} X_2^l, \\ x_2 &= X_2 + \sum_{k=2}^{\infty} \sum_{l=0}^{k} N_{2kl} X_1^{k-l} X_2^l, \end{aligned} \tag{2}$$

such that both N and N^{-1} are analytic functions in the neighbourhood D_0 of $X = 0$, for which the map $F = N^{-1} \circ f \circ N$: $\mathrm{R}^2 \to \mathrm{R}^2$ takes the simple form

$$\begin{aligned} X_1' &= U(X_1 X_2) X_1, \\ X_2' &= [U(X_1 X_2)]^{-1} X_2. \end{aligned} \tag{3}$$

The function U has as argument the product $X_1 X_2$ and it is analytic in a neighbourhood of $X_1 X_2 = 0$. Multiplying both equations in (3), we immediately verify that $X_1' X_2' = X_1 X_2$, so the map preserves this product. Thus the region where the map F is analytic is in fact the entire invariant region bounded by the invariant hyperbolae tangent to D_0. This region and its image under the transformation N is shown in fig. 1.

Let us now define the transformations

$$N_m = f^{-m} \circ N \circ F^m, \quad N_0 = N, \tag{4}$$

for all positive or negative m. Since N is analytic in D_0, N_{-m} is analytic in the region

$$D_m\colon F^m(D_0). \tag{5}$$

All the regions D_n have points in common, namely some neighbourhood of the origin as shown in fig. 2. Moreover N_0 and N_m coincide in the region where they both converge:

$$\begin{aligned} N_m &= f^{-m} \circ N_0 \circ F^m \\ &= N_0 \circ F^{-m} \circ N_0^{-1} \circ N_0 \circ F^m = N_0. \end{aligned} \tag{6}$$

The same is true for the transformations defined on any pair of regions D_m and $D_{m'}$, so we can define the extended normal form transformation to be

$$\mathbb{N} = \lim_{M \to \infty} \bigcup_{m=-M}^{M} N_m, \tag{7}$$

which will be analytic in the region

$$\mathbb{D} = \lim_{M \to \infty} \bigcup_{m=-M}^{M} D_m. \tag{8}$$

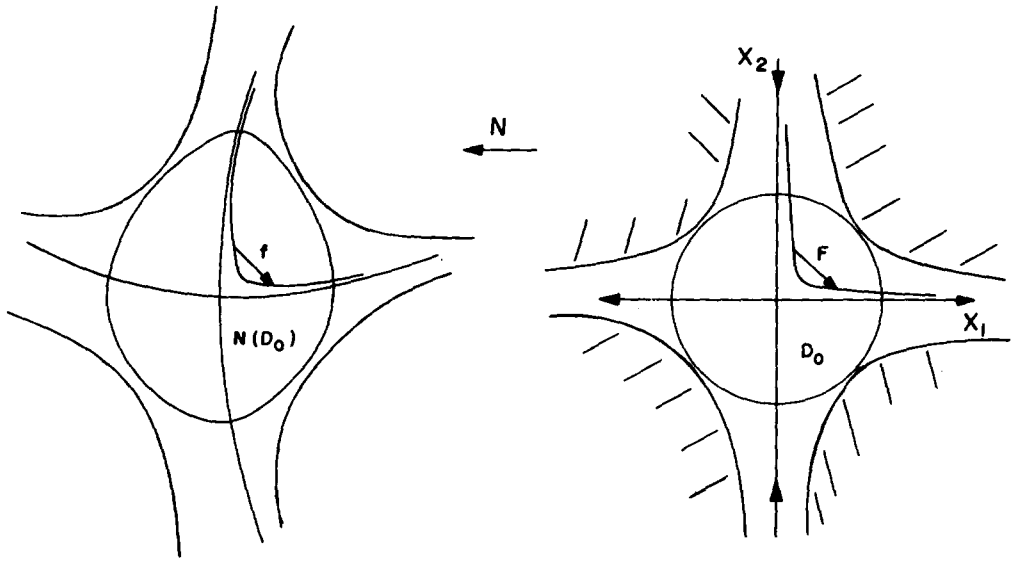

Fig. 1. The circle of convergence D_0 and the invariant hyperbolae which touch it are distorted by the normal form transformation N.

The Taylor series for each N_m at the origin will be identical with the series for N_0. We now need to show that the series for N_{-m} indeed converges in a region of D_m which extends far out of D_0. Moser proves convergence in a disc, so we can also take for D_0 a square of side $2X$ inscribed in this disc. We will need the fact that, if the complex Taylor series for $N_0(Z_1, Z_2)$ converges for particular values of $Z_1 = Z_{10}$ and $Z_2 = Z_{20}$, then it is absolutely convergent for $|Z_1| < |Z_{10}|$ and $|Z_2| < |Z_{20}|$. This theorem is analogous to the familiar result for functions of one variable (see for example Churchill's book [5]) and is proved in the same way. In the present case we thus establish the convergence of N_0 in D_{0c}, the direct product of the discs $|Z_1| < X$ and $|Z_2| < X$. The components of N_0 are therefore analytic within D_{0c}. The absence of singularities in this region can be verified to imply that $N_0 \circ F^{-m}$ has no singularities in $D_{mc} = F^m(D_{0c})$. Thus there are no singularities of the complexified functions N_{-m} within D_{mc}.

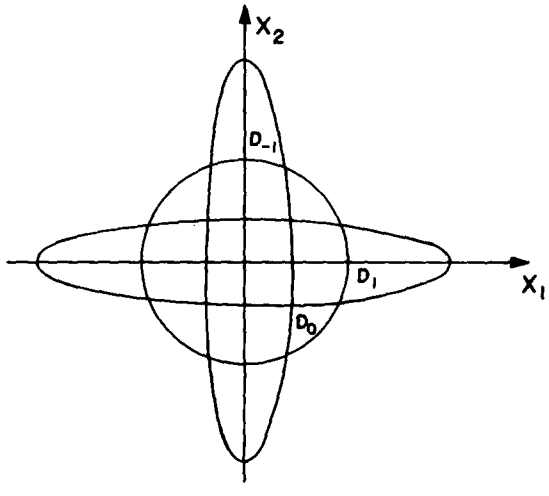

Fig. 2. All the images D_n of D_0 have a common intersection which includes the origin.

In the limit $X \to 0$ the transformation F is linear, in which case D_n is a rectangle with sides $2\lambda^m X$ and $2\lambda^{-m} X$. D_{mc} will then be the product of the pair of discs $|Z_1| < \lambda^m X$ and $|Z_2| < \lambda^{-m} X$. For finite X, D_{mc} will be distorted, so we define D'_{mc} to be the largest pair of discs $|Z_1| < X'_1$, $|Z_2| < X'_2$ which fits in D_{mc}. The absence of singularities in D'_{mc} entails the convergence of the

Taylor series

$$N_{-m}(Z_1, Z_2) = \sum_{\alpha} N_{-m}(Z_2) Z_1^{\alpha} \tag{9}$$

for all $(Z_1, Z_2) \in D'_{mc}$. Each function $N_{-m\alpha}(Z_2)$ is analytic for $|Z_2| \leq X'_2$. Expanding them in convergent Taylor series in Z_2 and introducing each one in (9), we obtain a convergent power series for $N_{-m}(Z)$, which coincides with the formal Taylor series. Thus the power series for $N_0(X)$ converges within the largest rectangle which can be inscribed in $F^m(D_0)$.

3. Homoclinic points and periodic orbits

The stable and the unstable manifolds of the map f are the images of the $X_1 = 0$ and the $X_2 = 0$ axes under the transformation $\mathbb{N}(X)$. In generic maps they may cross each other in *homoclinic points*, or there may be crossings with the stable or unstable manifolds of other hyperbolic points, i.e., *heteroclinic points*. As a consequence of the extension of the Birkhoff–Moser theorem in the previous section, we may calculate homoclinic points from the images of the two axes under $\mathbb{N}$. Computations of heteroclinic points demands the calculation of more than one normal form. Though it is not hard to compute some homoclinic points directly, by following orbits along the stable and unstable manifolds, the above method is the only one which provides the entire homoclinic orbit with uniform precision. We just need to follow the linear orbit of the normal coordinates $X'_j = [U(0)]^{\pm 1} X_j$ of the homoclinic point for positive and negative iterations, before transforming back to x. This last step is not even necessary close to the origin, since $\mathbb{N}$ is there asymptotic to the identity. The computational verification of these facts has been established [4] for the same map presented in section 4.

The normal form series also converges along the invariant hyperbolae close to the $X_1 = 0$ and $X_2 = 0$ axes. The images of these curves self-intersect near the homoclinic points. These self-intersections are not generally periodic points, but a simple argument due to Birkhoff [6] shows that they give rise to an infinite sequence of periodic points. Consider the point of self-intersection for a given curve; it will have many images under f along the invariant curve before the nth iteration takes it beyond the self-intersection. This situation is represented for the innermost curve of fig. 3(a). The average spacing between the points on the orbit diminishes continuously as we pick invariant curves which lie closer to the stable and the unstable manifolds, i.e. self-intersections which approach the homoclinic point. The reason is that the orbit then passes nearer to the fixed point, where it moves slower. There will therefore be curves for which it is only the $(n+1)$th point, which lies beyond the intersection (the outer curve in fig. 3(a)). The boundary between the two sets of curves has a self-intersection that is a periodic point of order n. By the same argument we find periodic orbits of arbitrarily high period. The next section presents periodic orbits calculated directly from the self-intersection of open invariant curves.

There are many other families of periodic orbits which accumulate on the homoclinic point. For instance there are the families based on the mutual intersections of a pair of invariant curves shown in fig. 3(b). In this case there are two conditions to be satisfied by two families of curves. Fig. 3(c) shows a periodic orbit based on three invariant curves. In general we can find periodic orbits bound to any number of invariant curves.

The larger the period of the orbit, the closer will the hyperbolae on which they lie be to the X axes. In this limit the map $F(X)$ becomes linear. Since the periodic points accumulate on the homoclinic point, their position is accurately given by a linearization of the normal form transformation $\mathbb{N}(X)$ around the homoclinic point. Combining both linearizations, we arrive at explicit linear equations for the periodic points, which are asymptotically exact in the limit of large periods. The situation is illustrated in fig. 4. The homoclinic point x^* has two images $(X_1^*, 0)$ and $(0, X_2^*)$

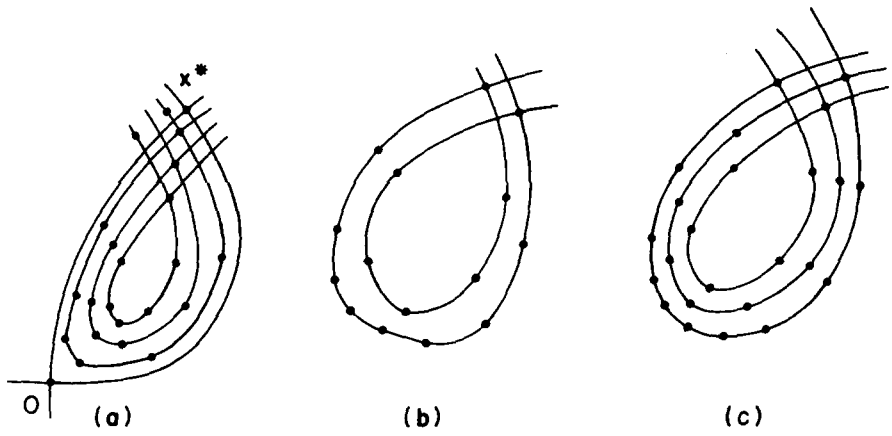

Fig. 3. (a) The three self-intersecting curves within the stable and the unstable manifolds are the images of invariant hyperbolae. There are five images of the point of intersection on the inner curve and six on the outer curve. The boundary curve supports a periodic orbit of period six. (b) Here the pair of curves supports a single periodic orbit of period fifteen. (c) A periodic orbit of period twenty-four, supported on three open invariant curves.

by the transformation $\mathbb{N}^{-1}$. Defining the restriction of $\mathbb{N}$ to a neighbourhood of $(X_1^*, 0)$ as $\mathbb{N}_1$ and the restriction to a neighbourhood of $(0, X_2^*)$ as $\mathbb{N}_2$, we see that the normal coordinates of the periodic point X_n, which moves on a single invariant curve, satisfies the equation

$$X_n = \mathbb{N}_2^{-1} \circ \mathbb{N}_1 \circ F^n(X_n). \tag{10}$$

The linearization of F^n is just

$$X' = \Lambda^n X = \begin{bmatrix} \lambda & 0 \\ 0 & \lambda^{-1} \end{bmatrix}^n X, \tag{11}$$

whereas the linearizations $D\mathbb{N}_j$, for which

$$x - x^* = D\mathbb{N}_1(X_1 - X_1^*, X_2) \tag{12}$$

and

$$x - x^* = D\mathbb{N}_2(X_1, X_2 - X_2^*) \tag{13}$$

are computed directly from the normal form series. Thus the required linearization of the right-hand side of (10) is

$$\begin{aligned} \mathbf{L}_n(X) &= D\left[\mathbb{N}_2^{-1} \circ \mathbb{N}_1 \circ F^n\right] X \\ &= (0, X_2^*) + (D\mathbb{N}_2)^{-1}(D\mathbb{N}_1) \\ &\quad \times \left[\Lambda^n X - (X_1^*, -0)\right], \end{aligned} \tag{14}$$

and the equation for the periodic point becomes

$$(\mathbf{L}_n - I) X_n = 0. \tag{15}$$

A periodic point based on J invariant curves is simply given by

$$\left(\prod_{j=1}^{J} \mathbf{L}_{n_j} - I \right) X_{n_j \cdots n_1} = 0. \tag{16}$$

Its period is $n_1 + \cdots + n_J$, but the asymptotic validity of (16) requires that all the $n_j \to \infty$. Despite appearances to the contrary it should be noted that (16) represents a pair of *inhomogeneous* equations, so that its solutions will be unique periodic points, except for circular permutations of the indices n_j.

It is interesting to observe that the presence of a countable infinity of periodic orbits is a consequence of the Smale–Birkhoff theorem [7] and

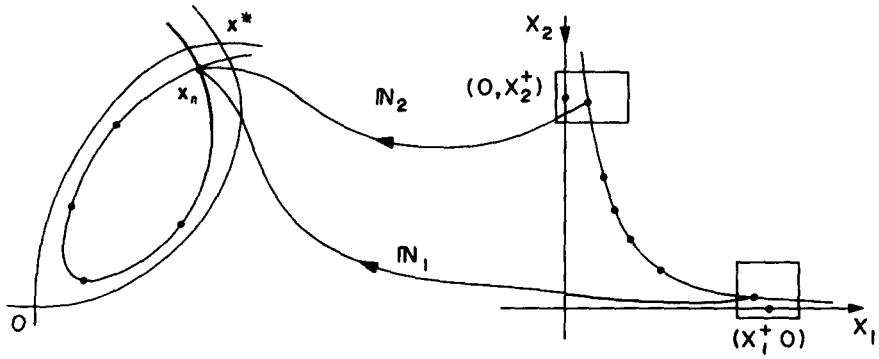

Fig. 4. $\mathbb{N}_1(X)$ and $\mathbb{N}_2(X)$ are respectively the restrictions of $\mathbb{N}(X)$ to the neighbourhoods of the pre-images of the homoclinic point $(X_1^*, 0)$ and $(0, X_2^*)$.

ultimately derives from the nonlinearity of the map f. It may seem strange that these orbits can be calculated from linear equations, but it must be borne in mind that the linearization is performed around the homoclinic point rather than the origin. Linear maps in which the orbits are 'folded back in' can be chaotic. This is the case of Arnol'd's cat map [2], a conservative map, or Smale's horseshoe [7], developed as a simplified model of homoclinic motion.

4. Computations for the quadratic map

The one-parameter family of maps,

$$\begin{aligned} y_1' &= y_1 \cosh\alpha + \left(y_2 - y_1^2\right)\sinh\alpha, \\ y_2' &= y_1 \sinh\alpha + \left(y_2 - y_1^2\right)\cosh\alpha, \end{aligned} \tag{17}$$

can be proved to be equivalent to all quadratic maps with a hyperbolic fixed point on the origin, just as the similar Henon map [8] is equivalent to all quadratic maps with an elliptic point on the origin. For small values of the parameter α, (17) is indeed equivalent to the Henon map, since it has a unique stable point away from the origin, but beyond $\alpha = \alpha_0 \simeq 1.8$ this point undergoes period doubling bifurcations, as described by Bountis [9]. A rotation of the axes by 45° takes (17) into the form

$$\begin{aligned} x_1' &= e^{\alpha}\left[x_1 - (x_1 + x_2)^2/4\right], \\ x_2' &= e^{-\alpha}\left[x_2 + (x_1 + x_2)^2/4\right], \end{aligned} \tag{18}$$

which has the form (1) with $\lambda = \exp\alpha$. The components of the map are quadratic, therefore the map and its inverse are entire functions. Hence we can apply the Birkhoff–Moser theorem to (18).

Introducing the normal form transformation (2) into (19) and defining the series

$$U^m(XY) = \lambda^m \sum_j \{U^m\}_{2j} (XY)^j, \tag{19}$$

we determine the coefficients for $N(X)$ and $U(XY)$ from the recursion relations

$$\begin{aligned} &\lambda U_{k-1}\delta_{k,2l+1} + \sum_{j=0} \lambda^{k-2l} N_{1,k-2j,l-j}\{U^{k-2l}\}_{2j} \\ &\quad -\lambda(N_{1kl} - R_{kl}/4) = 0, \\ &\lambda^{-1}(U^{-1})_{k-1}\delta_{k,2l-1} \\ &\quad + \sum_{j=0} \lambda^{k-2l} N_{2,k-2j,l-j}\{U^{k-2l}\}_{2j} \\ &\quad -\lambda^{-1}(N_{2kl} + R_{kl}/4) = 0, \end{aligned} \tag{20}$$

where

$$R_{kl}=2(T_{k-1,l-1}(1-\delta_{l,0})+T_{k-1,l}(1-\delta_{k,l}) + \sum_{j=0}^{l}\sum_{i=2}^{k-2} t_{k-i,l-j}t_{i,j}\theta(k-l-i+j) \times\theta(i-j), \tag{21}$$

$$T_{kl}=N_{1kl}+N_{2kl} \tag{22}$$

and

$$\theta(x)=\begin{cases}1, & x\geq 0,\\ 0, & x\leq 0.\end{cases} \tag{23}$$

The summations in (20) extend over all the indices compatible with the definition of the coefficients in (1), (2) and (19).

The coefficients $N_{1,k,2l+1}$ and $N_{2,k,2l-1}$ are indeterminate and have been chosen to be zero, as suggested by Birkhoff [1].

The stable and the unstable manifolds of $f(x)$ are the images of the $X_1=0$ and the $X_2=0$ axes respectively. The unstable manifold is given by

$$y_1=\tfrac{1}{2}\left[X_1+\sum_k (N_{1k0}+N_{2k0})X_1^k\right],$$
$$y_2=\tfrac{1}{2}\left[X_1+\sum_k (N_{1k0}-N_{2k0})X_1^k\right], \tag{24}$$

whereas the unstable manifold has equations

$$y_1=\tfrac{1}{2}\left[X_2+\sum_k (N_{1kk}+N_{2kk})X_2^k\right],$$
$$y_2=\tfrac{1}{2}\left[-X_2+\sum_k (N_{1kk}-N_{2kk})X_2^k\right]. \tag{25}$$

According to the recursion relations, we only need to calculate the coefficients N_{k0} and N_{kk} to obtain the manifolds and hence their intersection, the homoclinic point. Figs. 5(a) and 5(b) show respectively the stable and the unstable manifolds computed (a) directly (by iterating points on the manifolds close to the origin) and (b) by the normal

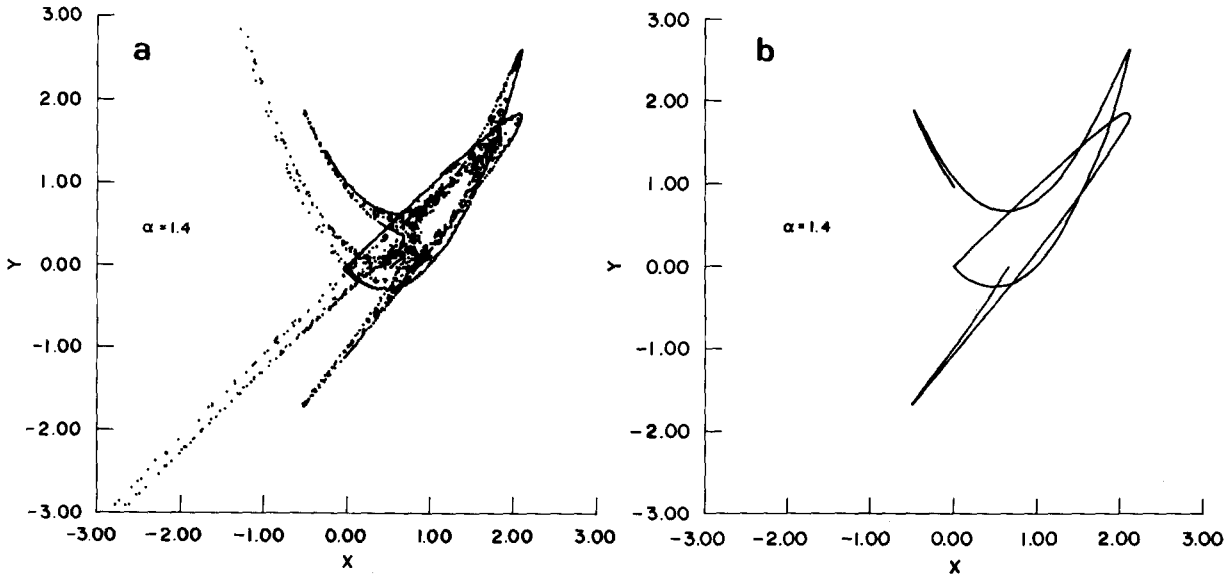

Fig. 5. (a) Points on the stable and unstable manifolds obtained by positive and negative iterations on the linear approximation of the manifolds very near the origin, for $\alpha = 1.4$. (b) The two separatrices calculated from the Birkhoff normal form up to twentieth order.

Table I

(y_{1a}, y_{2a}) are the coordinates of a homoclinic point computed from the intersection of the manifolds as in fig. 5(a). (y_{1b}, y_{2b}) are the coordinates according to the normal form as in fig. 5(b). N is the order of the normal form needed to obtain convergence to the numbers shown.

α	y_{1a}	y_{2a}	y_{1b}	y_{2b}	n
1.4	1.872 831	1.753 758	1.872 848	1.753 780	20
1.6	1.941 903	1.885 523	1.941 697	1.885 339	20
1.8	1.972 095	1.944 593	1.972 109	1.944 608	18
2.0	1.986 109	1.972 317	1.986 111	1.972 320	16
2.5	1.997 332	1.994 668	1.997 333	1.994 670	14
3.0	1.999 411	1.998 861	1.999 450	1.998 900	10
3.5	1.999 851	1.999 734	1.999 882	1.999 765	8
4.0	1.999 984	1.999 958	1.999 974	1.999 948	8
4.5	1.999 991	1.999 985	1.999 994	1.999 988	6
5.0	1.999 998	1.999 997	1.999 998	1.999 997	6
6.0	1.999 998	1.999 998	2.000 000	2.000 000	6
7.0	2.000 004	2.000 004	1.999 999	1.999 999	6

form. Table I shows the coordinates of the homoclinic point y^*, calculated for various parameters α. The last column specifies the number of terms needed for numerical convergence of the normal form at the homoclinic point. The small discrepancies between the two determinations of the homoclinic point can be mainly attributed to errors in the direct calculation, since the calculation of the periodic orbits using the normal form achieved a very high accuracy. Also we see that $y^* \to (2, 2)$ according to the normal form, which is the correct result [10]. These calculations have been published previously [4].

Tables II(a) and (b) give the y coordinates of two periodic orbits of period 10 computed for $\alpha = 2, 0$, in which the self-intersection of each in-

Table II

The y coordinates for two periodic orbits, each supported by a single self-intersecting curve, for $\alpha = 2, 0$. More significant figures were used for the starting point than shown here. The orbit of the first pair of coordinates (here abbreviated) will return to itself to a smaller accuracy than appears here.

y_1	y_2
(a)	
$0.198\,611\,241\,823\,560\,292\,018\,8910 \times 10^{1}$	$0.197\,232\,126\,893\,483\,724\,753\,2984 \times 10^{1}$
$0.318\,809\,6600 \times 10^{0}$	$-0.216\,906\,841 \times 10^{0}$
$0.441\,036\,0162 \times 10^{-1}$	$-0.421\,530\,6432 \times 10^{-1}$
$0.598\,839\,3361 \times 10^{-2}$	$-0.594\,842\,1359 \times 10^{-2}$
$0.825\,351\,4661 \times 10^{-3}$	$-0.794\,973\,9740 \times 10^{-3}$
$0.219\,403\,4624 \times 10^{-3}$	$0.240\,689\,3965 \times 10^{-7}$
$0.825\,351\,4661 \times 10^{-3}$	$0.795\,655\,1790 \times 10^{-3}$
$0.598\,839\,3361 \times 10^{-2}$	$0.598\,428\,2215 \times 10^{-2}$
$0.441\,036\,0162 \times 10^{-1}$	$0.440\,981\,9199 \times 10^{-1}$
$0.318\,809\,6600 \times 10^{0}$	$0.318\,545\,6835 \times 10^{0}$
$0.198\,611\,241\,823\,560\,292\,018\,8910 \times 10^{1}$	$0.197\,232\,126\,893\,483\,724\,753\,1040 \times 10^{1}$
(b)	
$0.175\,575\,961\,920\,591\,819\,067\,4168 \times 10^{1}$	$0.133\,717\,626\,525\,034\,643\,3144\,0536 \times 10^{1}$
$0.274\,769\,9430 \times 10^{0}$	$-0.199\,076\,1270 \times 10^{0}$
$0.378\,943\,7345 \times 10^{-1}$	$-0.364\,513\,3246 \times 10^{-1}$
$0.515\,404\,2148 \times 10^{-2}$	$-0.510\,189\,4257 \times 10^{-2}$
$0.790\,312\,4077 \times 10^{-3}$	$-0.601\,272\,7174 \times 10^{-3}$
$0.790\,312\,4077 \times 10^{-3}$	$0.601\,897\,3111 \times 10^{-3}$
$0.515\,404\,2148 \times 10^{-2}$	$0.512\,845\,8408 \times 10^{-2}$
$0.378\,943\,7345 \times 10^{-1}$	$0.378\,873\,1600 \times 10^{-1}$
$0.274\,769\,9430 \times 10^{0}$	$0.274\,574\,6486 \times 10^{0}$
$0.175\,575\,9619 \times 10^{1}$	$0.174\,551\,5575 \times 10^{1}$
$0.175\,575\,961\,920\,591\,819\,067\,4168 \times 10^{1}$	$0.133\,717\,626\,525\,034\,643\,144\,0611 \times 10^{1}$

Table III
Coordinates y and X of periodic points of period 10(a), 15(b) and 20(c) calculated from explicit linear equations.

(a) $n = 10$	
$y_1 = 1.986\,112\,41$	$y_2 = 1.972\,321\,23$
$(y_1)^{10} = 1.986\,112\,17$	$(y_2)^{10} = 1.972\,321\,03$
$X_1 = 0.996\,026\,780 \times 10^{-8}$	$X_2 = 4.823\,237\,520$
(b) $n = 15$	
$y_1 = 1.986\,112\,42$	$y_2 = 1.972\,321\,26$
$(y_1)^{15} = 1.986\,112\,42$	$(y_2)^{15} = 1.972\,321\,29$
$X_1 = 0.452\,195\,465 \times 10^{-12}$	$X_2 = 4.832\,375\,35$
(c) $n = 20$	
$y_1 = 1.986\,112\,42$	$y_2 = 1.972\,321\,26$
$(y_2)^{20} = 1.986\,112\,42$	$(y_2)^{20} = 1.972\,321\,29$
$X_1 = 0.205\,296\,424 \times 10^{-16}$	$X_2 = 4.832\,375\,35$

variant curve was found by Newton's method. The first pair of coordinates y_{10} give the values computed from the normal form, whereas the last pair are those of $f_{10}(y_{10})$. In spite of the instability of the map, we achieve periodicity within 21 significant figures! Each orbit is based on a single invariant curve, the first point in table II(a) being close to the homoclinic point in table I. The first point of table II(b) lies in the neighbourhood of the next intersection of the stable and unstable manifolds, belonging to a different homoclinic orbit. It is hard to go beyond this simplest pair of homoclinic orbits, because of the very large numbers involved in the normal form transformation, as one moves out along the stable and the unstable manifolds. We have not been able to calculate the more complicated homoclinic orbits and the periodic points which accumulate on them.

Finally, in table III(a) we present the same periodic point of table II(a), together with its tenth iterate, calculated from the explicit formula (15). Table III(b) and III(c) supply the coordinates of periodic points of period 15 and 20 in the same family. Notice the asymptotic improvement in accuracy from $n = 10$ to $n = 15$. For high order periodic points the difficulty of verification becomes that of controlling errors in the multiple iteration of the map.

5. Conclusion

We have shown that the Birkhoff normal form provides the basis for precise calculation of homoclinic orbits and the periodic orbits of arbitrarily high period, which accumulate on them. This technique can evidently be extended to the calculation of heteroclinic points and their satellite periodic orbits and to the calculation of homoclinic or heteroclinic points of time periodic Hamiltonian systems with one degree of freedom. Indeed Moser's proof applies directly to these systems, while the convergence of the normal form for a map relies on the possibility of interpolating a periodic system for any map.

Outside of the direct realm of application of the Birkhoff–Moser theorem, we conjecture that normal forms for unstable equilibria of autonomous Hamiltonian systems with two freedoms, for which there are no small denominators, may also permit the calculation of homoclinic orbits. In particular this is the case of the system with one real pair and one imaginary pair of eigenvalues: its Poincaré map near the origin has exactly the form described in the foregoing discussion.

As a method for the calculation of periodic points, the self-intersection of invariant curves reduces the problem to a one-dimensional search. In this respect it resembles the method of Greene [1], which applies to reversible maps, i.e. those which can be decomposed as the product of two inversions. The map (17) belongs to this class and the orbits based on a single invariant curve or on a pair of curves are symmetric. For these orbits Greene's method is just as good. Orbits based on three invariant curves come in symmetry pairs (one of which is shown on fig. 3(e)). These cannot be calculated by Greene's method, though in its

turn it has the advantage of not being limited to unstable points close to a homoclinic point. Of course, the explicit asymptotic formulae for high period orbits can only be obtained from the Birkhoff normal form.

Acknowledgements

We gratefully acknowledge a helpful discussion with A. Douady and the financial support of CNPq, FAPESP and FINEP. R. Douady thanks IMPA in Rio de Janeiro for its hospitality.

References

[1] G.D. Birkhoff, Acta Math. 43 (1920) 1.
[2] V.I. Arnol'd, Geometrical Methods in the Theory of Ordinary Differential Equations (Springer, New York, 1982).
[3] J. Moser, Commun. Pure and Appl. Math. IX (1956) 673.
[4] A.M. Ozorio de Almeida, R.J.S.B. Coutinho and G.L. da Silva Ritter, Rev. Bras. Fis. 15 (1985) 60.
[5] R.V. Churchill, Complex Variables and Applications (McGraw-Hill, New York, 1960).
[6] G.D. Birkhoff, Acta Math. 50 (1927) 359.
[7] J. Guckenheimer and P. Holmes, Nonlinear Oscillations, Dynamical Systems and Bifurcations of Vector Fields (Springer, New York, 1983).
[8] M. Henon, Q. Appl. Math. 27 (1969) 291.
[9] T.C. Bountis, Physica 3D (1981) 577.
[10] G.L. da Silva Ritter, Master's Thesis, Unicamp (1986).
[11] J.M. Greene, J. Math. Phys. 20 (1979) 1183.